

Probing the Heavy Quark Content of the Photon
Using b Tagging at High Energy $e\gamma$ and e^+e^- Colliders

Michael A. Doncheski*, Stephen Godfrey and
K. Andrew Peterson†

Ottawa-Carleton Institute for Physics

Department of Physics, Carleton University, Ottawa CANADA, K1S 5B6

We suggest a method for probing the quark content of the photon using b tagging at high energy e^+e^- and $e\gamma$ colliders. We find that heavy quark tagging provides a sensitive and effective probe of the quark content of the photon especially in the low x -region where the various models differ the most. This process is complementary to others that have been studied in the literature and can contribute to more precise determinations of quark and gluon distributions inside the photon.

PACS numbers: 12.15.Ji, 14.80.Er, 12.50.Fk

Typeset Using *REVTEX*

*Present address: Department of Physics, Pennsylvania State University, Mont Alto, PA 17237
USA

†Present address: Department of Physics, Memorial University of Newfoundland, St. John's, NF,
Canada, A1B 3X7

I. INTRODUCTION

There is a growing interest in the hadronic content of the photon [1] as both a test of QCD and as a background to precision measurements of electroweak parameters. In fact, some photoproduction processes are dominated by the hadronic interactions of photons in certain regions of phase space [2,3]. Although there have been several theoretical calculations of the hadronic content of the photon [4–7], at present the experimental data [8] are not adequate to significantly constrain theory. Recently a number of papers have appeared which present methods of extracting the gluonic component of the photon [2,9,10]. In particular, the potential of $e\gamma$ colliders for the study of the hadronic content of the photon has been studied by several authors [2,9]. (Such colliders, where high energy e^+e^- colliders are converted into $e\gamma$ colliders, are receiving considerable interest for the phenomenology that may be studied in $e\gamma$ collisions.) However, these analysis have concentrated on dijet production in $e\gamma$ collisions where it is difficult to isolate the effect of the gluon and quark distributions. A good determination of the quark content of the photon is therefore needed to test the various models of the photon structure functions and is essential for the extraction of the gluon content of the photon. In this paper we present a novel method of measuring the heavy quark content of the photon using hard scattered b -quarks at e^+e^- and $e\gamma$ colliders. We find that by using b tagging to probe quark distributions inside the photon it should be possible to differentiate between the various existing sets of photon distribution functions using a 500 GeV e^+e^- collider operating in $e\gamma$ mode.

Recently, there has been some related work on heavy quark production. In the context of leptonproduction on a proton, in Ref. [11] Olness and Riemersma pointed out that there are advantages to using both a fixed flavor scheme (in which, *e.g.*, the b -quark is not considered to be a constituent) [12] and a variable flavor scheme (in which, *e.g.*, the b -quark may or may not be considered a constituent depending on energy scale) [13]. Although these works all deal with leptonproduction on a proton, many of the ideas will apply, with suitable modifications, to leptonproduction on a photon. In Ref. [14], heavy quark production in two

photon processes at an e^+e^- collider is discussed; although some mention is made of the heavy quark content of the photon, the bulk of the analysis deals with the production of heavy quark pairs *via* $\gamma\gamma$, γg and gg fusion. Finally, Laenen and Riemersma [15] present a calculation of heavy quark production in $e\gamma$ collisions using a fixed flavor scheme; as we consider the heavy quark as being a constituent of the photon, our approach should be considered to be complementary to that of Ref. [15].

II. CALCULATION

We are interested in the measurement of $f_{b/\gamma}(x, Q^2)$ which contributes to the process $e + \gamma \rightarrow e + b + \text{jet}$ via the subprocess $e + b \rightarrow e + b$ which can be written

$$\sigma(e\gamma \rightarrow eb \text{ jet}) = \int dx f_{b/\gamma}(x, Q^2) \hat{\sigma}(eb \rightarrow eb). \quad (1)$$

This process is shown in Fig. 1. It is straightforward to calculate the amplitude for the subprocess $e + b \rightarrow e + b$, and the squared and summed/averaged matrix element is given by:

$$\begin{aligned} |\overline{\mathcal{M}}|^2 = & \\ & 32\pi^2\alpha^2 \left\{ [(\hat{s} - m_b^2)^2 + (\hat{u} - m_b^2)^2] \left[\frac{Q_b^2 Q_e^2}{\hat{t}^2} + \frac{2Q_e Q_b g_V^e g_V^b}{s_W^2 c_W^2 \hat{t}} \frac{(\hat{t} - M_Z^2)}{(\hat{t} - M_Z^2)^2 + \Gamma_Z^2 M_Z^2} \right. \right. \\ & \left. \left. + \frac{((g_V^e)^2 + (g_A^e)^2)((g_V^b)^2 + (g_A^b)^2)}{s_W^4 c_W^4} \frac{1}{(\hat{t} - M_Z^2)^2 + \Gamma_Z^2 M_Z^2} \right] \right. \\ & + 2m_b^2 \hat{t} \left[\frac{Q_b^2 Q_e^2}{\hat{t}^2} + \frac{2Q_e Q_b g_V^e g_V^b}{s_W^2 c_W^2 \hat{t}} \frac{(\hat{t} - M_Z^2)}{(\hat{t} - M_Z^2)^2 + \Gamma_Z^2 M_Z^2} \right. \\ & \left. \left. + \frac{((g_V^e)^2 + (g_A^e)^2)((g_V^b)^2 - (g_A^b)^2)}{s_W^4 c_W^4} \frac{1}{(\hat{t} - M_Z^2)^2 + \Gamma_Z^2 M_Z^2} \right] \right. \\ & \left. + [(\hat{s} - m_b^2)^2 - (\hat{u} - m_b^2)^2] \left[\frac{2Q_e Q_b g_A^e g_A^b}{s_W^2 c_W^2 \hat{t}} \frac{(\hat{t} - M_Z^2)}{(\hat{t} - M_Z^2)^2 + \Gamma_Z^2 M_Z^2} \right. \right. \\ & \left. \left. + \frac{4g_V^e g_A^e g_V^b g_A^b}{s_W^4 c_W^4} \frac{1}{(\hat{t} - M_Z^2)^2 + \Gamma_Z^2 M_Z^2} \right] \right\}. \end{aligned}$$

In the above equation, $s_W = \sin \theta_W$ and $c_W = \cos \theta_W$ with θ_W being the weak angle; $g_{V,A}^{e,b}$ are the vector and axial vector couplings of the electron and b -quark to the Z^0 , respectively, chosen such that $g_A^e = 1/4$ (this fixes the remainder of the couplings unambiguously). Also, $Q_{e,b}$ are the electric charges of the electron and b -quark, respectively.

In some sense the process $e\gamma \rightarrow eb$ jet can be regarded as an approximation to the direct (pointlike) process $e\gamma \rightarrow ebb$ in analogy to the effective W approximation or the Weiszäcker-Williams approximation. With appropriate kinematic cuts to ensure that we are describing the same kinematic region, the p_T distributions of the outgoing b in the two approaches closely resemble each other, as demonstrated in Fig. 2. In addition, contributions from the process $eg \rightarrow ebb$, with the gluon coming from the hadronic structure of the photon, are similarly contained in our resolved photon contribution *via* the Altarelli-Parisi evolution of the distribution functions. When we consider backgrounds we must take care so as not to double count these contributions.

To determine whether the process is viable as a probe of the quark content of the photon we must include detector acceptances and consider the possible backgrounds. Fortunately the signature for the process is quite distinct, a single b balanced against the beam electron and possibly hadronic jet remnants of the photon. For b detection we use a typical LEP detector acceptance for b 's of $|\cos \theta| < 0.85$ and assume a b detection efficiency of 50%. The jet remnants will generally go down the beam so when considering backgrounds we can veto events with jets detected above some minimum angle. One sees that the crux of the analysis is to determine whether the signal is overwhelmed by backgrounds.

To illustrate the background contributions we take as an example b -quark production at a 500 GeV $e\gamma$ collider where we have folded in the photon spectrum for the backscattered laser and use (to be specific) the Duke and Owens photon structure functions [4]. The general properties of the other cases we will consider are the same. Possible backgrounds are shown in Fig. 3. They can be divided into direct processes (Fig. 3a),

$$e^+ + e^- \rightarrow b + \bar{b} \quad (3)$$

$$e^+ + e^- \rightarrow \gamma + b + \bar{b} \quad (4)$$

$$e + \gamma \rightarrow e + b + \bar{b} \quad (5)$$

$$e + \gamma \rightarrow \nu + b + \bar{c} \quad (6)$$

singly resolved (Fig. 3b)

$$e + [g]_\gamma \rightarrow e + b + \bar{b} \quad (7)$$

$$e + [g]_\gamma \rightarrow \nu + b + \bar{c} \quad (8)$$

and doubly resolved (Fig. 3c)

$$[g]_\gamma + [g]_\gamma \rightarrow b + \bar{b} \quad (9)$$

$$[q]_\gamma + [\bar{q}]_\gamma \rightarrow b + \bar{b} \quad (10)$$

where we used the notation $[p]_\gamma$ to represent parton p 's content in the photon. We include detector acceptance cuts of $|\cos \theta_{eb}| < 0.85$ for the b , where θ_{eb} is the angle between b and the beam direction, the observed electron (or positron) is at least 10° from the beam and all particles not to be detected must be within 10° of the beam except for neutrinos.

We start with the two processes already mentioned above, $e\gamma \rightarrow e b \bar{b}$ (eqn. 5) and $e[g]_\gamma \rightarrow e b \bar{b}$ (eqn. 7). The pointlike process $e\gamma \rightarrow e b \bar{b}$ contains a collinear divergence arising from the internal b -quark line which is also included in the process $e\gamma \rightarrow e b$ jet. This divergence must therefore be first subtracted as described in Ref. [13,16] before including it as a background. Likewise, the process $e[g]_\gamma \rightarrow e b \bar{b}$, *i.e.*, with the gluon coming from the hadronic structure of the photon, is similarly, to some approximation, contained in our resolved photon contribution *via* the Altarelli-Parisi evolution of the distribution functions. A similar collinear subtraction must be made if $e[g]_\gamma \rightarrow e b \bar{b}$ is to be considered a correction to our result. We find that, after making the required collinear subtraction, both processes $e\gamma \rightarrow e b \bar{b}$ (direct) and $e g \rightarrow e b \bar{b}$ (once resolved) contribute negligibly in the kinematic region under study.

In the remaining background discussions we are concerned with decay chains that might be mistaken for the signal. In particular, in the processes listed in eqns. (3)-(10) heavy quarks are pair produced which could lead to the situation where the \bar{b} (or \bar{c}) decays semileptonically and only an electron is seen by the detector. Clearly, this is expected to be rather unlikely given that all decay products, both leptonic and hadronic, are expected to be boosted in the same direction given the relatively large energy of the produced quarks. The likelihood of these events is further reduced given the small branching fractions for these decay chains.

Keeping this in mind we start by describing the possible direct process backgrounds. The first two backgrounds are only relevant to the e^+e^- cases involving Weizsäcker-Williams photons. The background $e^+ + e^- \rightarrow b + \bar{b}$ is negligible compared to $e^+ + e^- \rightarrow b + \bar{b} + \gamma$ even though it is technically of lower order in coupling. This is because the b and \bar{b} come out back-to-back with high p_T and are therefore very distinct because the decay products of the \bar{b} are boosted along the \bar{b} direction making it very unlikely that the electron is seen in the detector while the hadronic remnants go down the beampipe. The second direct background, $e^+ + e^- \rightarrow b + \bar{b} + \gamma$, will also turn out to be unimportant in the relevant kinematic region once the \bar{b} is allowed to decay and cuts are imposed so that only the e^- and b are observed. The third direct background, $e + \gamma \rightarrow e + b + \bar{b}$, can contribute in two ways. In the first, the beam electron is observed in the detector and the decay products of the \bar{b} are not, while in the second the beam electron goes down the beampipe but the electron from \bar{b} decay is seen in the detector. As discussed above, the situation in which the beam electron is hard scattered into the detector is approximated by our signal and corrections to the signal, due to this process after subtracting the collinear divergence, are found to be negligible in this kinematic region (this process was calculated numerically using helicity amplitude techniques). The other possibility, where the beam electron goes down the beampipe and is not seen in the detector, can be well described using the Weizsäcker-Williams approximation and the subprocess $\gamma + \gamma \rightarrow b + \bar{b}$ (the subprocess cross section can be extracted from, *e.g.*, Ref. [17]). The final direct process which could contaminate the

signal is the charged current process, $e + \gamma \rightarrow \nu + b + \bar{c}$ Ref. [18]; here the electron seen in the detector comes from the decay of the \bar{c} .

We next consider the singly resolved backgrounds. As discussed above, if the beam electron is hard scattered into the detector, the first of the singly resolved backgrounds, $e + [g]_\gamma \rightarrow e + b + \bar{b}$, (again, we use helicity amplitude techniques to calculate this process numerically), is approximated by our signal; corrections to our result in the appropriate kinematic region, after the necessary collinear subtraction has been made, are found to be negligible. It is also possible that the beam electron goes down the beam pipe, in which case this background can be well described in the Weizsäcker-Williams approximation with the subprocess $\gamma + g \rightarrow b + \bar{b}$ (this cross section can also be extracted from Ref. [17] by carefully modifying couplings and color factors). Also, the charged current process $e + [g]_\gamma \rightarrow \nu + b + \bar{c}$ can also contribute to the background if the \bar{c} decays leptonically and the resulting electron is observed in the detector; with some care, this subprocess can be extracted from Ref. [18].

Finally, we consider the doubly resolved backgrounds where the photon from the beam electron contributes a parton from its hadronic structure. Since the parton model of photon structure is defined for real photons only, it is appropriate to use the Weizsäcker-Williams approximation, with the subprocesses $[g]_\gamma + [g]_\gamma \rightarrow b + \bar{b}$ and $[q]_\gamma + [\bar{q}]_\gamma \rightarrow b + \bar{b}$, to calculate these backgrounds (see Ref. [19] for the cross sections).

The largest of the backgrounds are displayed in Fig. 4. The p_T (of the b quark) distributions of the two charged current processes have, as expected, rather long tails due to the large mass of the exchanged particle. These p_T distributions are, however, several orders of magnitude smaller than our signal, and do not appear on our plot for the scale chosen. The remaining subprocesses fall off rapidly with p_T of the b quark; although they may produce many events at small p_T , they are safely negligible for $p_T > 40 \text{ GeV}$. We did not include charge identification of the leptons since we include both b and \bar{b} production in our distributions and estimates of event numbers as they both make equal contributions. This approach also eliminates the complexities of $B^0 - \bar{B}^0$ mixing in the analysis.

III. RESULTS

Having convinced the reader that the signal we are studying is distinct and clean of backgrounds we proceed to examine the sensitivity of various kinematic distributions to different structure function parameterizations for a number of collider possibilities. We consider a group of the existing sets of photonic parton distributions that appear in the literature, namely the set of Duke and Owen (DO) [4], the set of Drees and Grassie (DG) [5], the set 1 of Abramowicz, Charchula and Levy (LAC) [6] and the leading order set of Glück, Reya and Vogt (GRV) [7].

We first considered the LEP e^+e^- collider at CERN upgraded in luminosity using the Weizsäcker-Williams photon distributions with the $e\gamma$ cross sections to obtain numerical results. The cross section for the signal is expected to be between 0.108 pb (GRV) to 0.220 pb (LAC). An order of magnitude improvement in the LEP luminosity, resulting in $1 \text{ fm}^{-1}/\text{year}$, would yield 108-220 b 's per year or of order 50-100 reconstructed b 's once efficiencies are included. This small number of events is unlikely to offer an improvement over existing estimates of the b content of the photon. At the LEP200 e^+e^- collider the cross section is expected to be 0.047 pb (GRV) to 0.092 pb (LAC) which would yield roughly 40 b 's or 20 reconstructed b 's for the total integrated luminosity of 500 pb^{-1} . Clearly a higher energy and higher luminosity collider is needed.

We therefore turn to the proposed higher energy NLC e^+e^- collider in both e^+e^- mode and $e\gamma$ mode with $\sqrt{s}=500 \text{ GeV}$ and very high luminosity yielding of order $50 \text{ fb}^{-1}/\text{year}$. In the e^+e^- mode we fold in the Weizsäcker-Williams effective photon distribution and the $e\gamma$ mode we fold in the backscattered laser photon spectrum.

First, consider the e^+e^- configuration. The cross section is expected to be between 14 fb (GRV) and 24 fb (LAC). Given $50 \text{ fb}^{-1}/\text{yr}$ of luminosity, we expect 700 to 1200 events per year, and after the 50% b reconstruction efficiency, of order 500 reconstructed b 's per year. This will allow a measurement of the b -quark distribution in the photon at some level, but even so, more events are desirable. The p_T distribution of the b -quark is shown in Fig. 5a

for various sets of photon distribution functions.

Lastly, consider a $\sqrt{s} = 500$ GeV linear e^+e^- collider configured as an $e\gamma$ collider through the use of a backscattered laser. In this situation, we expect a cross section of between 68 fb (GRV) and 138 fb (LAC), with all backgrounds smaller by at least 2 orders of magnitude after the implementation of the cuts described above. This gives a total of 3400 to 6900 events per year, and after the b reconstruction efficiency, there will still be 2000-3000 events per year to analyze. The p_{T_b} distribution for the signal is shown in Fig. 5b for various choices of photon distributions.

Having established that only the two cases involving an NLC can provide a useful measurement of the b -quark content of the photon (*i.e.*, large enough signal combined with manageable backgrounds), we consider useful experimental measurements.

Before proceeding we point out a subtlety that should be mentioned but that we will ignore. The subtlety is related to the fact that the parton model (including the distribution function model of the hadronic structure of the photon) implicitly assumes that the constituents are massless (or, that the mass of the partons is small relative to all energy scales in the problem, and so can be safely ignored). As we are producing a massive b -quark, the minimum \hat{s} is of order m_b^2 , and it is not necessarily possible to ignore the initial b -quark mass compared to all mass scales, namely $\sqrt{\hat{s}}$. In practice it turns out that our results are only sensitive to a finite m_b for two cases; at the lower energy colliders where the statistics are insufficient to make a meaningful measurement and for the low x region of $d\sigma/dx$ distributions (where, following the standard parton model notation, $\hat{s} = xys$ and $p_b = xyp_{\bar{e}}$, y is the fraction of the electron's momentum carried by the photon, and x is (nominally) the fraction of the photon's momentum carried by the b -quark). In the latter case the uncertainties are only in the lowest x region where the statistical errors will still overwhelm the uncertainties in our definition of the scale.

In the figures that follow, only the estimated **statistical** uncertainties are included in the error bars, so that the error bars shown will slightly underestimate the actual errors.

A physically measurable quantity is the ratio of the initial b -quark energy or momentum

to the beam energy. This will generally be closely related to $\tau = xy$, and the conversion is easily calculated. We show, in Fig. 6a, the number of events *vs.* τ for various photon distribution functions in the $e\gamma$ case. The largest differences in the models are in the lowest τ bins where the event numbers are largest. Considering only the lowest τ bin and using the Duke-Owens results to estimate the error we obtain a statistical error of roughly 2.5%. Thus, using only the lowest τ bin for the measurement, and the higher τ bins as a normalization, it will be quite easy to distinguish between the various distribution functions. Fig. 6b shows the same distribution in the e^+e^- case. Here, the conclusion is not so clear, due to relatively larger error bars, but it should be possible to distinguish between LAC, DO/DG and GRV, though it may not be possible to distinguish DO from DG.

Finally we show, in Fig. 6a ($e\gamma$) and in Fig. 6b (e^+e^-) the distribution of event numbers in x . This distribution will be useful if one can tag the electron which provides the Weizsäcker-Williams photon (allowing a complete reconstruction of the $e\gamma$ initial state, including y), or in the $e\gamma$ case if one can deconvolute the τ distribution knowing the parton level cross section and the laser backscattered photon spectrum. As with the τ distribution, the large x bins can be used to fix the normalization of the distribution while the lowest x bin can be used to provide information on the b -quark distribution in the photon. Similar conclusions can be reached here as well: in the $e\gamma$ case, it should be possible to distinguish between the various distribution functions, while in the e^+e^- case it should be possible to distinguish between LAC, DO/DG and GRV (though possibly not between DO and DG).

IV. CONCLUSIONS

In this paper we proposed using high p_T b -quarks as a means of determining the heavy quark content of the photon. We have shown that the process $e + \gamma \rightarrow e + b + X$ provides a clean method of extracting the quark content of the photon and can distinguish between the different models in the literature. The subprocess we examined was $e + b \rightarrow e + b$ where the beam electron undergoes a hard scatter from a resolved b in the photon, in essence

Rutherford scattering off a photon target. The signal for the process is quite distinct; all backgrounds can be eliminated by insisting that only the scattered b -quark balanced against the beam electron be observed and imposing a minimum p_T cut on the b to eliminate the remaining direct and once resolved $b\bar{b}$ production.

It is clear that this reaction will allow a good determination of the quark content of the photon. In the low x -regions of the distributions, where the models differ the most, typical uncertainties are roughly 2.5% for the $e\gamma$ colliders. This is more than adequate to distinguish between different models. For the e^+e^- cases the statistics are poorer and do not offer quite as good a measurement, though valuable information can be extracted from these data. One could also use this approach to study the charmed quark content of the photon [22]. The c -quark content of the photon is roughly four times as large as the b -quark content due to the different quark electric charges. However, since charmed mesons are more difficult to reconstruct, the b -quark gives a cleaner signal. The process we have proposed is complementary to others that have been studied in the literature and can contribute to more precise determinations of quark and gluon distributions inside the photon. Along with other processes considered elsewhere it is clear that an $e\gamma$ collider is an ideal facility for studying the hadronic content of the photon.

ACKNOWLEDGMENTS

SG thanks Rohini Godbole for helpful discussions in the early stages of this work and Richard Hemingway for helpful conversations. MAD thanks Manuel Drees for many enlightening discussions during the course of this work. This research was supported in part by the Natural Sciences and Engineering Research Council of Canada (NSERC), and the work of MAD was supported in part by an NSERC Canada International Fellowship.

REFERENCES

- [1] E. Witten, *Nucl. Phys.* **B120**, 189(1977).
- [2] O.J. Éboli, M.C. Gonzalez-Garcia, F. Halzen, and S.F. Novaes, *Phys. Lett.* **B301**, 115 (1993).
- [3] M. Drees, M. Krämer, J. Zunft, P.M. Zerwas, *Phys. Lett.* **B306**, 371 (1983); P. Chen, T.L. Barklow, and M.E. Peskin, *Phys. Rev.* **D49**, 3209 (1994); M. Drees and R.M. Godbole, DESY Report DESY 92-044 (1992); O.J. Éboli, M.C. Gonzalez-Garcia, F. Halzen, and S.F. Novaes, *Phys. Rev.* **D47**, 1889 (1993).
- [4] D.W. Duke and J.F. Owens, *Phys. Rev.* **D26**, 1600 (1982).
- [5] M. Drees and K. Grassie, *Z. Phys.* **C28**, 451 (1985); M. Drees and R. Godbole, *Nucl. Phys.* **B339**, 355 (1990).
- [6] H. Abramowicz, K. Charchula, and A. Levy, *Phys. Lett.* **B269**, 458 (1991).
- [7] M. Glück, E. Reya and A. Vogt, *Phys. Lett.* **B222**, 149 (1989); *Phys. Rev.* **D45**, 3986 (1992); *Phys. Rev.* **D46**, 1973 (1992).
- [8] CELLO Collaboration (H.-J. Behrend, *et al.*), *Phys. Lett.* **126B**, 391 (1983); PLUTO Collaboration (Ch. Berger, *et al.*), *Phys. Lett.* **142B**, 111 (1984); *Nucl. Phys.* **B281**, 365 (1987); JADE Collaboration (W. Bartel, *et al.*), *Z. Phys.* **C24**, 231 (1984); TASSO Collaboration (M. Althoff, *et al.*), *Z. Phys.* **C31**, 527 (1986); TPC/Two-Gamma Collaboration (H. Aihara, *et al.*), *Phys. Rev. Lett.* **58**, 97 (1987); *Z. Phys.* **C34**, 1 (1987); AMY Collaboration (T. Sasaki, *et al.*), *Phys. Lett.* **B252**, 491 (1990); B.J. Kim *et al.*, *Phys. Lett.* **B325**, 248 (1994); H1 Collaboration (I. Abt, *et al.*), *Phys. Lett.* **B314**, 436 (1993); ALEPH Collaboration (D. Buskulic *et al.*) *Phys. Lett.* **B313**, 509 (1993); OPAL Collaboration (R. Akers, *et al.*), *Z. Phys.* **C61**, 199 (1994); L.E. Gordon and J.K. Storrow, hep-ph/9607370.
- [9] A.C. Bawa and W.J. Stirling, *Z. Phys.* **C57**, 165 (1993).

- [10] M. Glück, E. Reya, and A. Weber, *Phys. Lett.* **B298**, 176 (1993).
- [11] F. I. Olness and S. T. Riemersma, *Phys. Rev.* **D51**, 4746 (1995).
- [12] E. Laenen, S. Riemersma, J. Smith and W. L. van Neerven, *Nucl. Phys.* **B392**, 162 (1993); 229 (1993).
- [13] M. A. G. Aivazis, F. I. Olness and W.-K. Tung, *Phys. Rev.* **D50**, 3085 (1994); M. A. G. Aivazis, J. C. Collins, F. I. Olness and W.-K. Tung, *Phys. Rev.* **D50**, 3102 (1994).
- [14] K. Hagiwara, M. Tanaka, I. Watanabe and T. Izubuchi, *Phys. Rev.* **D51**, 3197 (1995).
- [15] E. Laenen and S. Riemersma, *Phys. Lett.* **B376**, 169 (1996).
- [16] J. Blümlein and G. A. Schuler, in *Research Directions for the Decade*, Proceedings of the 1990 Summer Study on High Energy Physics, ed. E. L. Berger, World Scientific, Singapore, pg. 552.
- [17] S. J. Brodsky, T. Kinoshita and H. Terazawa, *Phys. Rev.* **D4**, 1532 (1971).
- [18] G. Jikia, *Nucl. Phys.* **B374**, 83 (1992).
- [19] V. D. Barger and R. J. N. Phillips, *Collider Physics*, Addison-Wesley Publishing Company, Redwood City, California, 1987.
- [20] I. F. Ginzburg, G. L. Kotin, V. G. Serbo and V. I. Telnov, *Nucl. Instr. Meth.* **205**, 47 (1983); I. F. Ginzburg, G. L. Kotkin, S. L. Panfil, V. G. Serbo and V.I. Telnov, *Nucl. Instr. Meth.* **219**, 5 (1984).
- [21] S. Dawson, *Nucl. Phys.* **B249**, 42(1985).
- [22] See for example, D. Miller, *Proceedings of the XVI International Symposium on Lepton-Photon Interactions*.

FIGURES

FIG. 1. Feynman diagram for the process $e\gamma \rightarrow eb + X$.

FIG. 2. Comparison of direct $e + \gamma \rightarrow e + b + \bar{b}$ (dashed curve), $e + [g]_\gamma \rightarrow e + b + \bar{b}$ (dotdashed curve) and the sum (dotted curve) to the signal process $e + \gamma \rightarrow e + b + X$ (solid curve). All curves correspond to a 500 GeV e^+e^- collider operating in $e\gamma$ mode. For the signal, $e[b]_\gamma \rightarrow eb$, (solid curve) we require that the final state electron and b -quark be seen, θ_e more than 10° from the beampipe and $|\cos\theta_b| < 0.85$; for the direct processes, there is an additional requirement, $|\cos\theta_{\bar{b}}| > 0.85$.

FIG. 3. Diagrams for background processes. (a) Direct contributions; (b) Singly resolved contributions; (c) Doubly resolved contributions.

FIG. 4. p_{T_b} distribution for the signal (solid line) and the most dangerous backgrounds: $\gamma + [g]_\gamma \rightarrow b + \bar{b}$ (rightmost dotted line), $\gamma + \gamma \rightarrow b + \bar{b}$ (rightmost dashed line), $[g]_\gamma + [g]_\gamma \rightarrow b + \bar{b}$ (leftmost dotted line), $[q]_\gamma + [\bar{q}]_\gamma \rightarrow b + \bar{b}$ (leftmost dashed line), $e^+ + e^- \rightarrow \gamma + b + \bar{b}$ (dotdashed line). These all make use of the Duke and Owens photon distribution functions (where appropriate), and are for a 500 GeV e^+e^- collider operating in $e\gamma$ mode.

FIG. 5. p_{T_b} distribution for the signal with LAC (solid line), GRV (dashed line), DO (dotted line) and DG (dotdashed line) distributions, using $Q^2 = \hat{s}$ at (a) a 500 GeV e^+e^- collider and (b) a 500 GeV e^+e^- collider configured as an $e\gamma$ collider.

FIG. 6. Event number *vs.* τ for a 500 GeV e^+e^- collider assuming $L=50 \text{ fb}^{-1}$ operating in (a) $e\gamma$ mode and (b) e^+e^- mode, using the four different sets of photon distribution functions. The solid curve is for LAC set 1, the dashed curve for GRV, the dotted curve for DO and the dotdashed curve for DG.

FIG. 7. Event number *vs.* x for a 500 GeV e^+e^- collider assuming $L=50 \text{ fb}^{-1}$ operating in (a) $e\gamma$ mode and (b) e^+e^- mode, using the four different sets of photon distribution functions. The solid curve is for LAC set 1, the dashed curve for GRV, the dotted curve for DO and the dotdashed curve for DG.

This figure "fig1-1.png" is available in "png" format from:

<http://arxiv.org/ps/hep-ph/9407348v2>

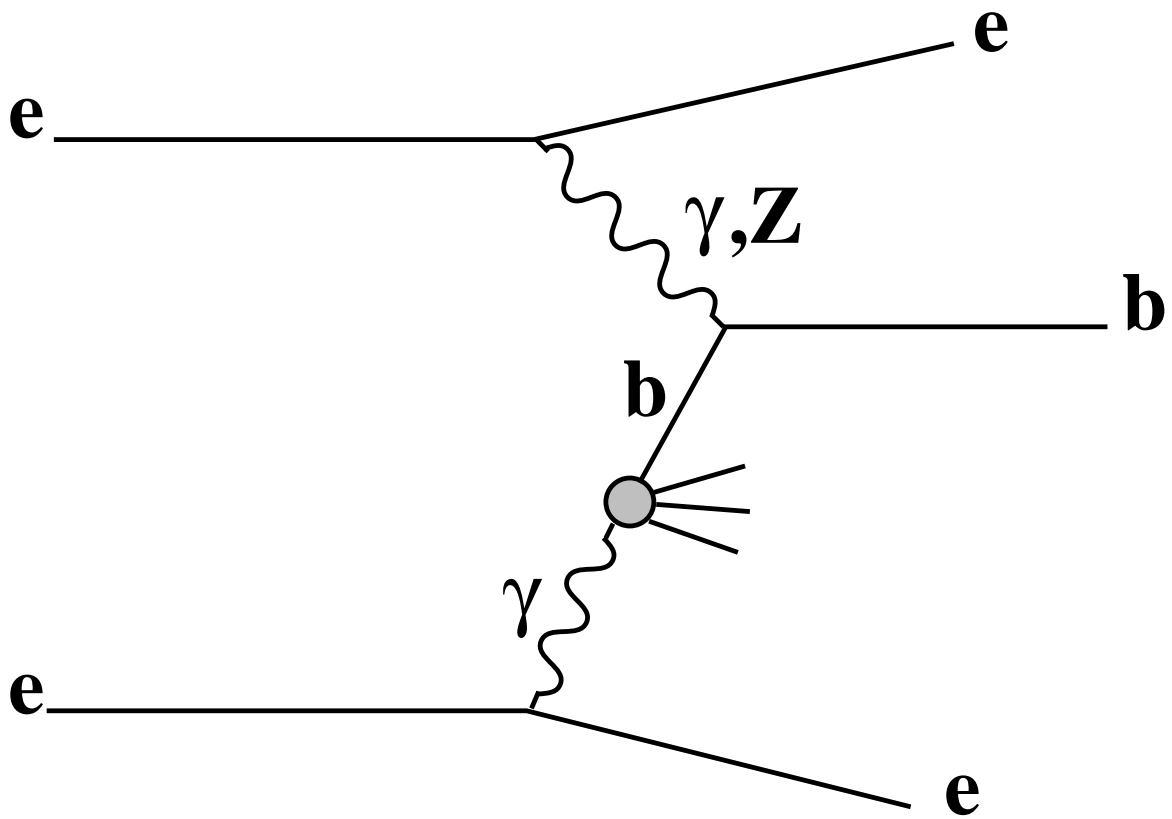


FIGURE 1

This figure "fig2-1.png" is available in "png" format from:

<http://arxiv.org/ps/hep-ph/9407348v2>

This figure "fig3-1.png" is available in "png" format from:

<http://arxiv.org/ps/hep-ph/9407348v2>

This figure "fig4-1.png" is available in "png" format from:

<http://arxiv.org/ps/hep-ph/9407348v2>

This figure "fig1-2.png" is available in "png" format from:

<http://arxiv.org/ps/hep-ph/9407348v2>

This figure "fig2-2.png" is available in "png" format from:

<http://arxiv.org/ps/hep-ph/9407348v2>

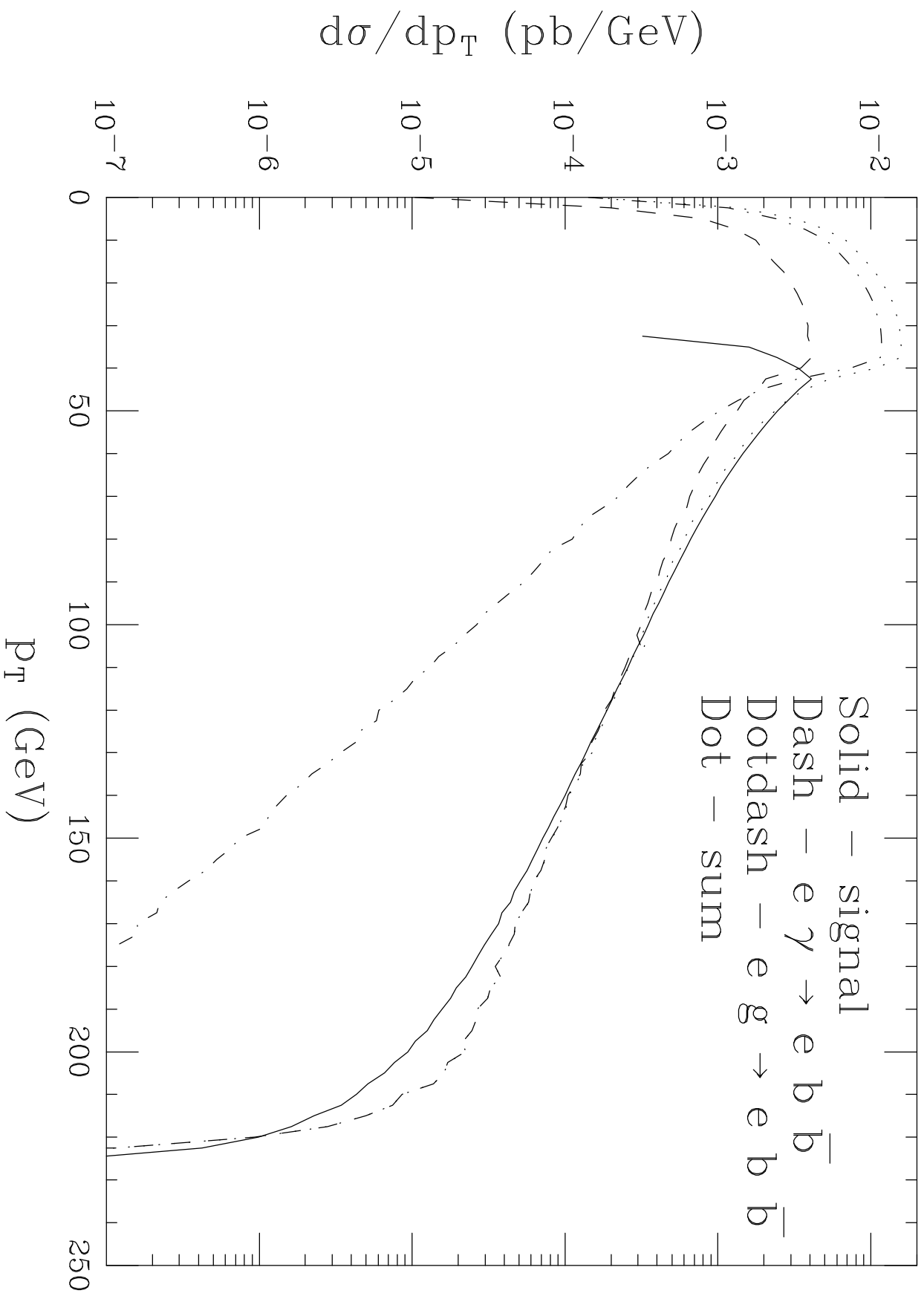


Figure 2

This figure "fig3-2.png" is available in "png" format from:

<http://arxiv.org/ps/hep-ph/9407348v2>

This figure "fig4-2.png" is available in "png" format from:

<http://arxiv.org/ps/hep-ph/9407348v2>

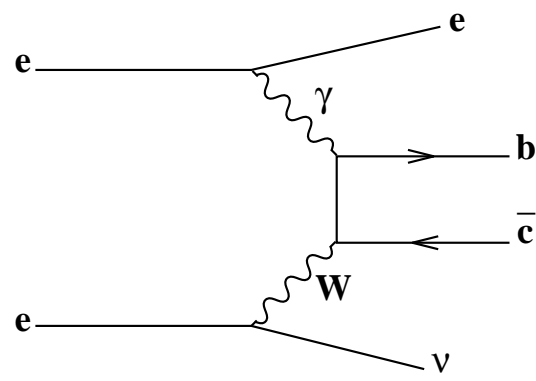
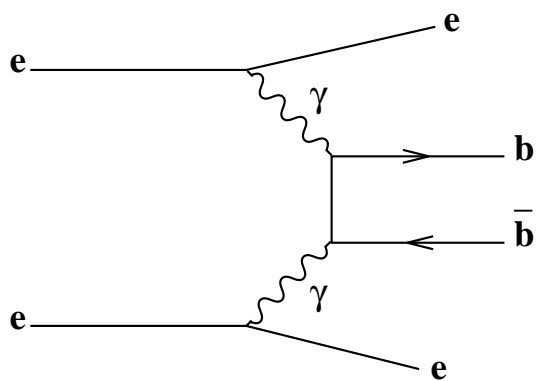
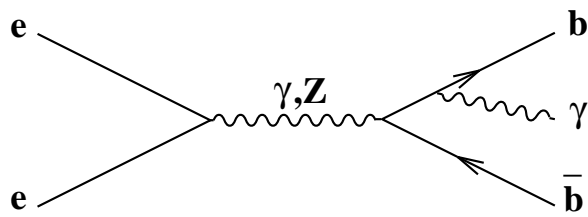
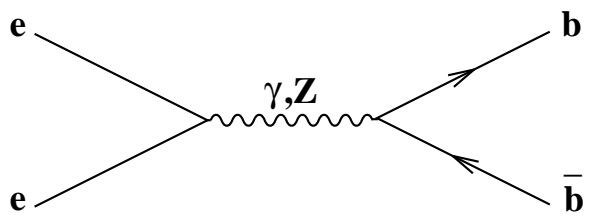
This figure "fig2-3.png" is available in "png" format from:

<http://arxiv.org/ps/hep-ph/9407348v2>

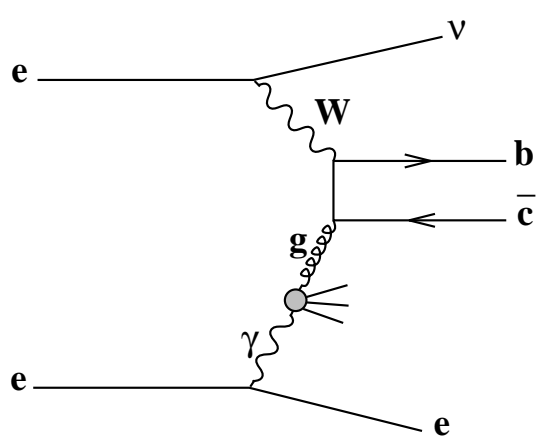
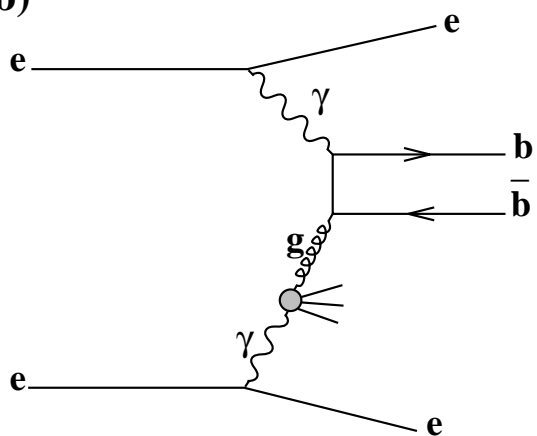
This figure "fig3-3.png" is available in "png" format from:

<http://arxiv.org/ps/hep-ph/9407348v2>

a)



b)



c)

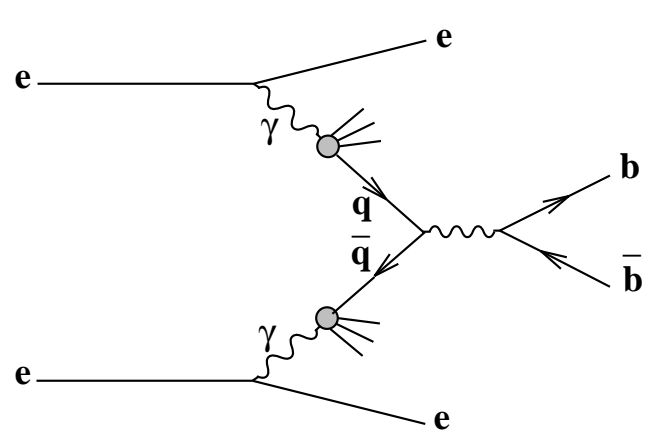
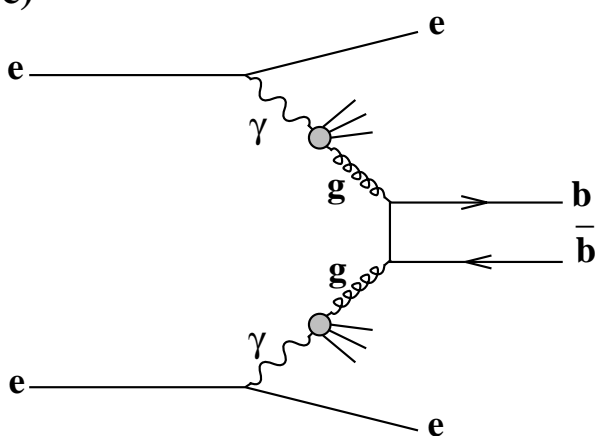


FIGURE 3

This figure "fig4-3.png" is available in "png" format from:

<http://arxiv.org/ps/hep-ph/9407348v2>

This figure "fig2-4.png" is available in "png" format from:

<http://arxiv.org/ps/hep-ph/9407348v2>

This figure "fig3-4.png" is available in "png" format from:

<http://arxiv.org/ps/hep-ph/9407348v2>

Figure 4

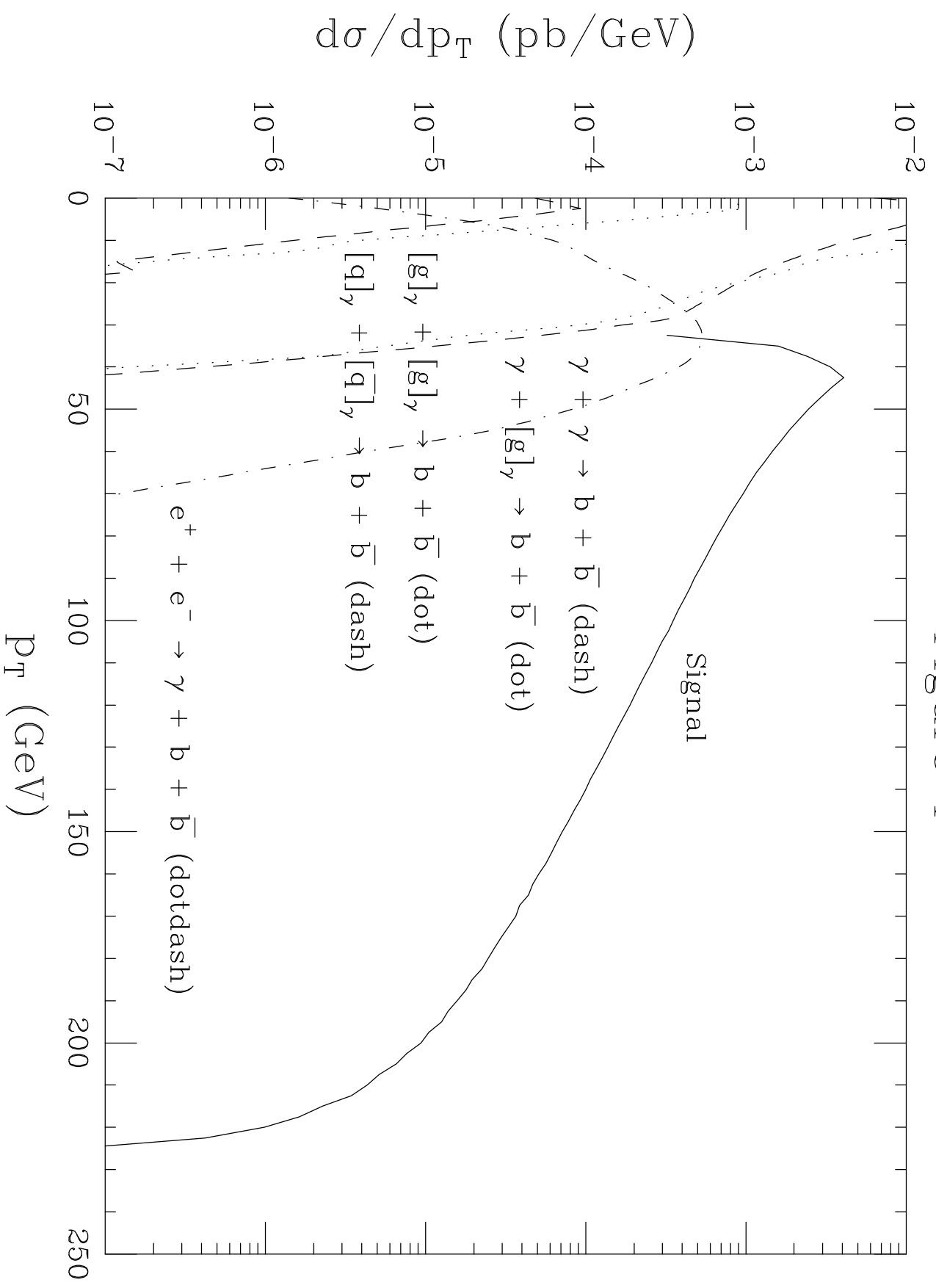


Figure 5a

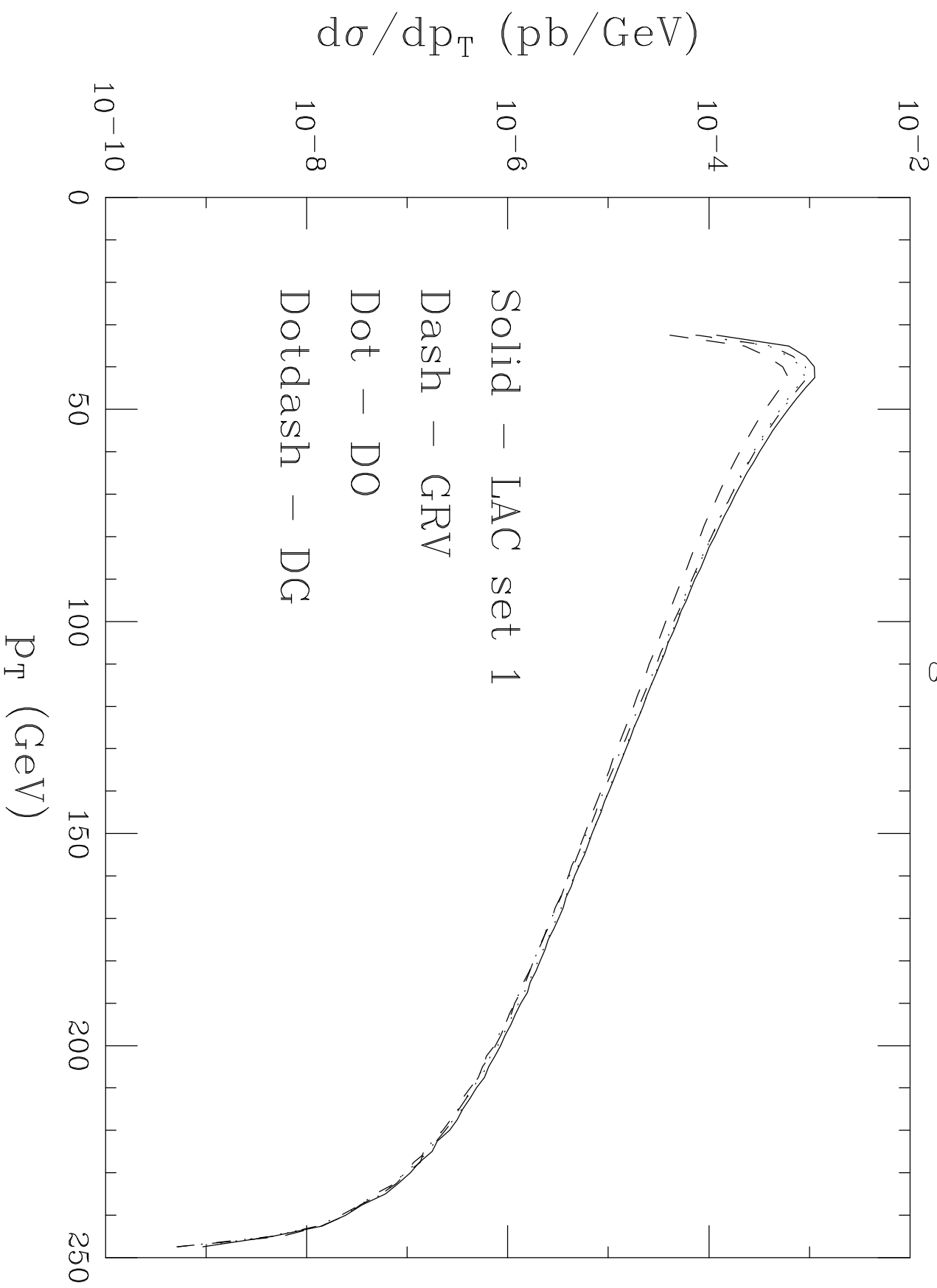


Figure 5a

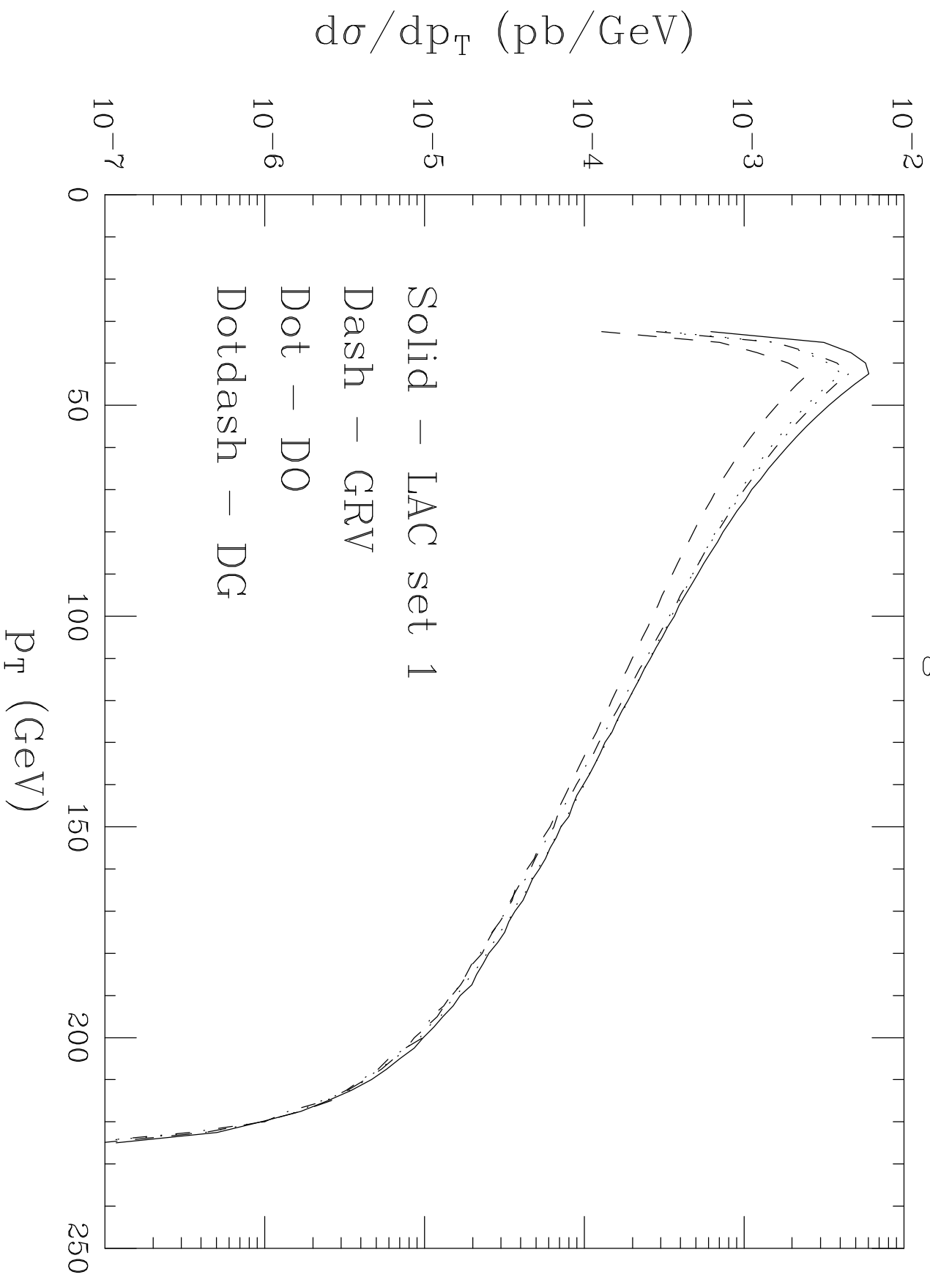


Figure 6a

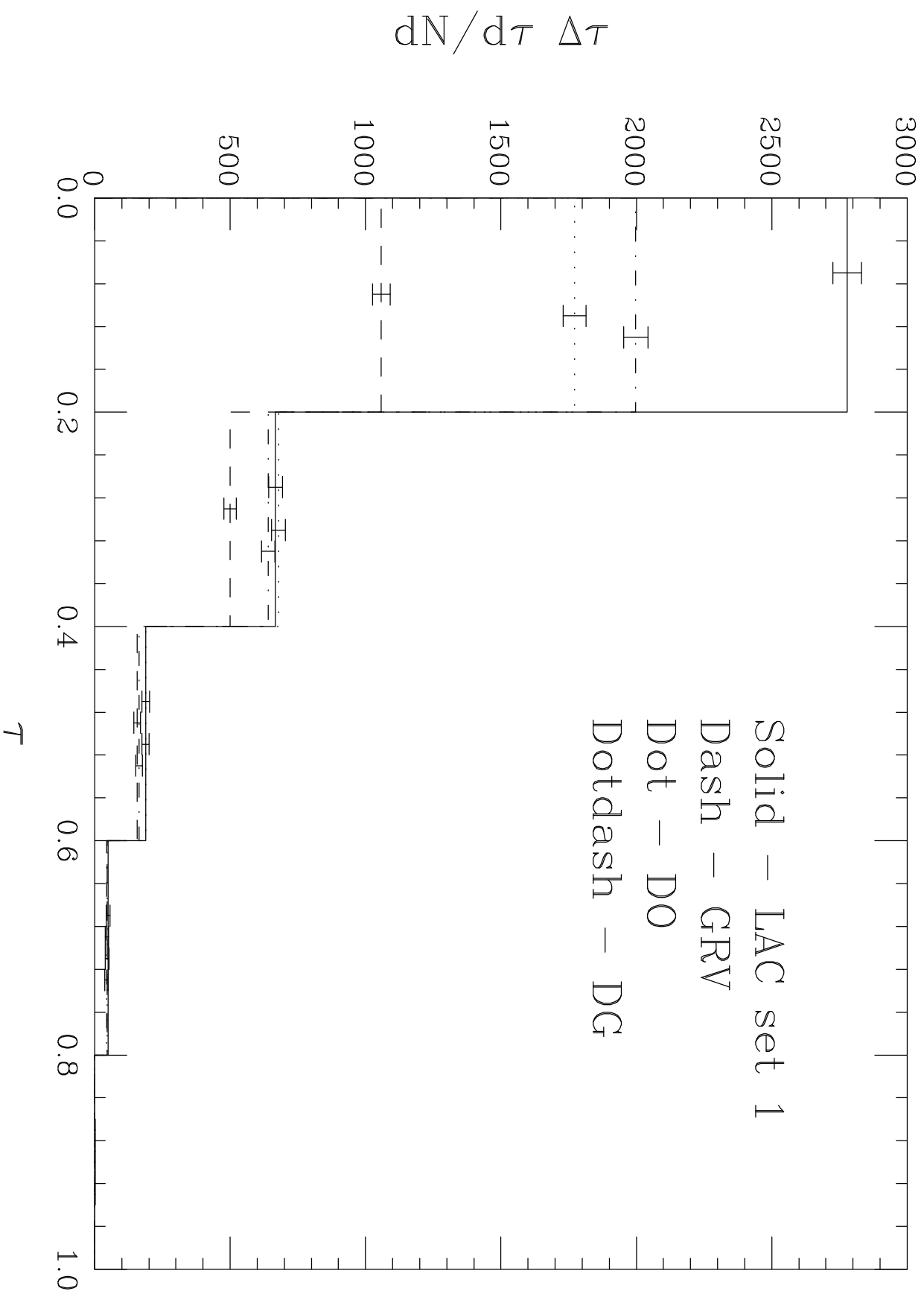


Figure 6b

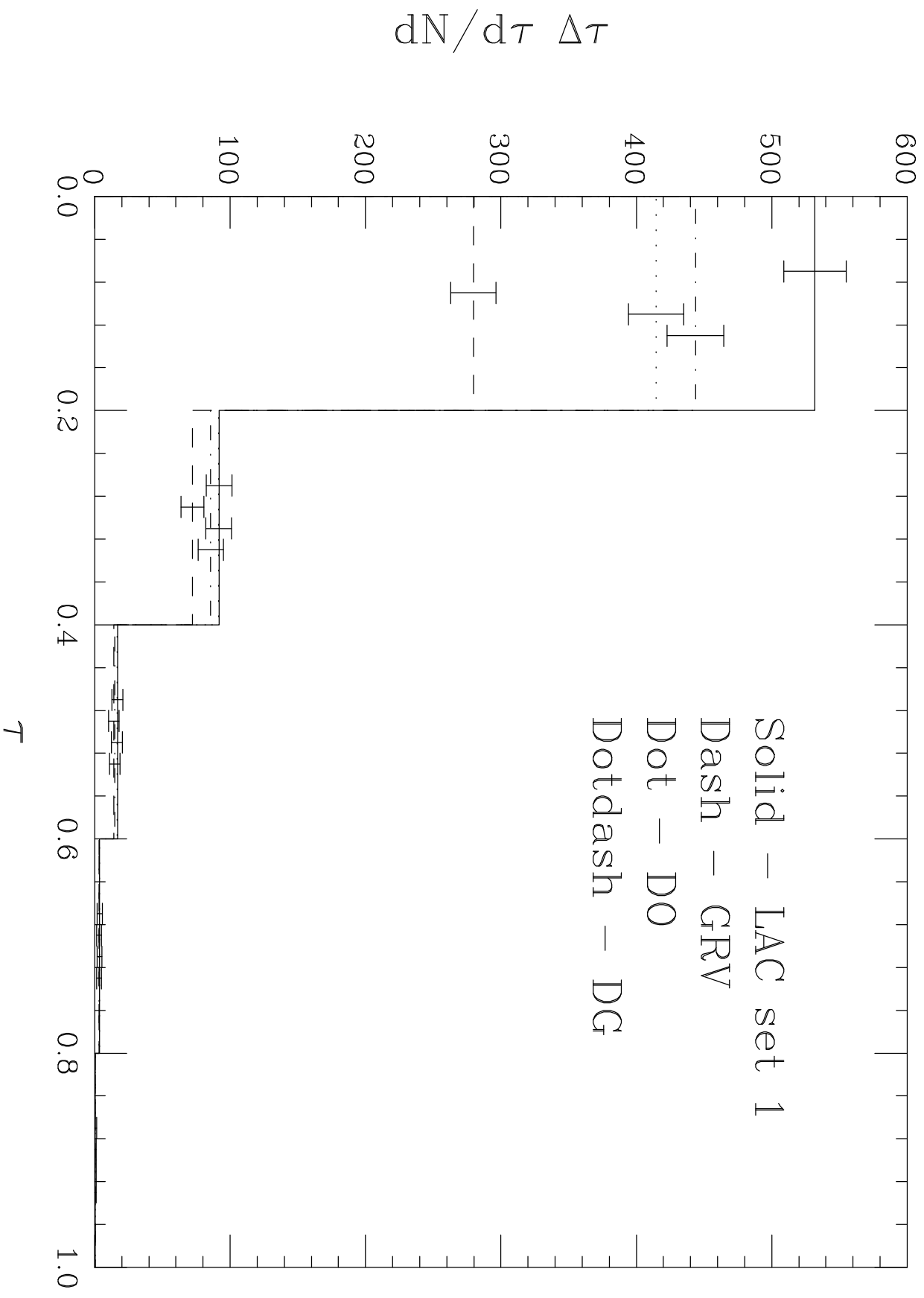


Figure 7a

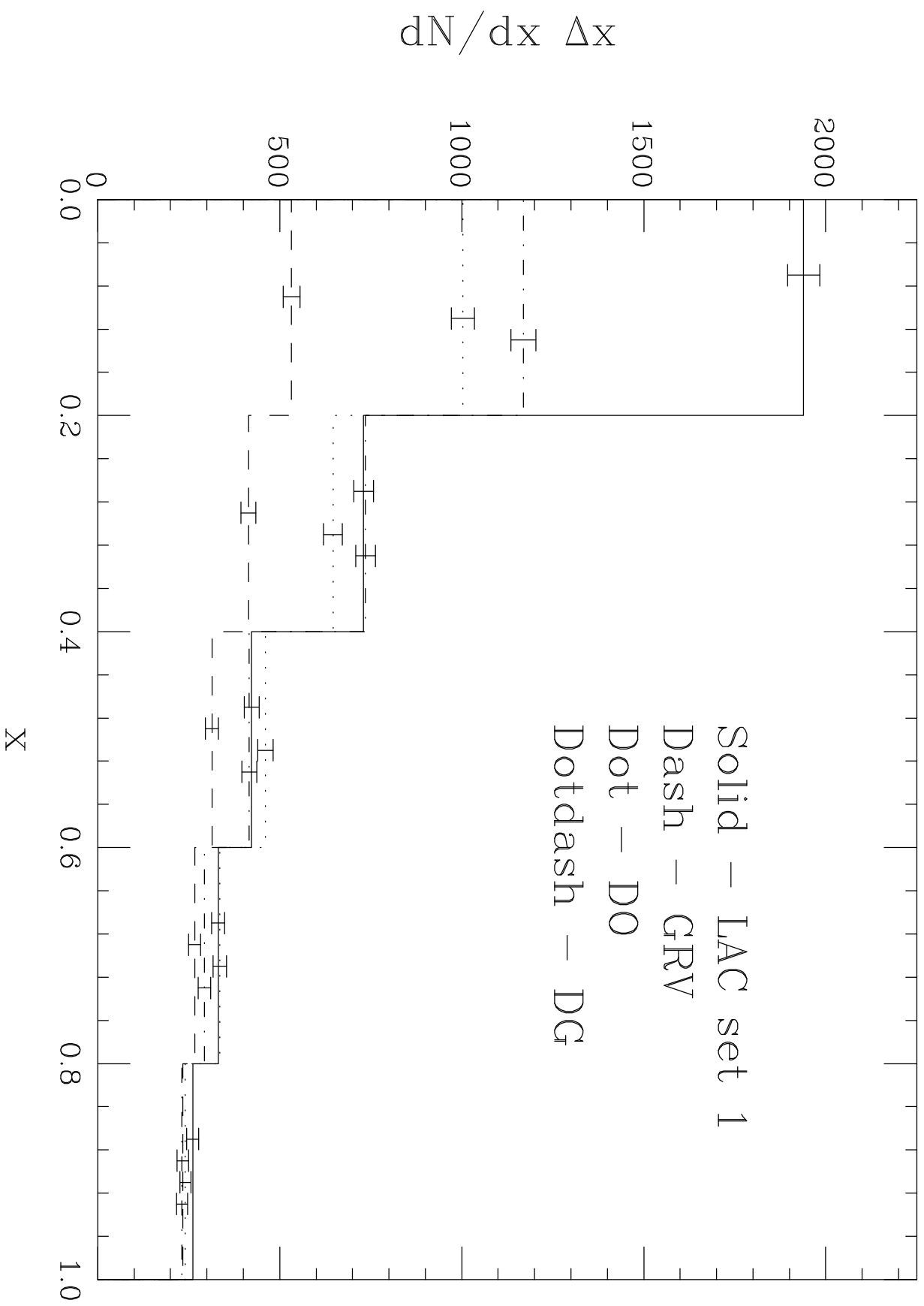


Figure 7b

